Journal of The Electrochemical Society, **148** (9) A994-A998 (2001)
0013-4651/2001/148(9)/A994/5/$7.00 © The Electrochemical Society, Inc.

Structural Changes (Degradation) of Oxysulfide $LiAl_{0.24}Mn_{1.76}O_{3.98}S_{0.02}$ Spinel on High-Temperature Cycling

Yang-Kook Sun,[a,*,z] Gyeong-Su Park,[b] Yun-Sung Lee,[c] Masaki Yoashio,[c,*] and Kee Suk Nahm[d,*]

[a]*Department of Industrial Chemistry, Hanyang University, Seoul 133-791, Korea*
[b]*Samsung Advanced Institute of Technology, Analytical Engineering Laboratory, Suwon 440-600, Korea*
[c]*Department of Applied Chemistry, Saga University, Saga 840, Japan*
[d]*School of Chemical Engineering and Technology, Chonbuk National University, Chonju 561-756, Korea*

The structural integrity of the oxysulfide material, $LiAl_{0.24}Mn_{1.76}O_{3.98}S_{0.02}$ before and after charge-discharge cycling at high temperature was studied by X-ray diffraction and high-resolution transmission electron microscopy. The rock salt phase Li_2MnO_3 which is associated with capacity loss has been detected at the surface of the oxysulfide particles in the electrode cycled in the 4 V region at 80°C. The small structural degradation of the new oxysulfide material may be responsible for the excellent cyclability of the oxysulfide spinel at high temperature over the 4 V region.
 [DOI: 10.1149/1.1391270]

Manuscript submitted June 29, 2000; revised manuscript received March 17, 2001. Available electronically August 3, 2001.

$LiMn_2O_4$ spinels have generated great interest as the most promising cathode materials (positive electrodes) for lithium secondary batteries, due to their high energy density, low cost, abundance, and nontoxicity. $Li_xMn_2O_4$ ($x = 1$) has a cubic spinel structure with space group symmetry $Fd3m$ in which the Li^+ and $Mn^{3+/4+}$ ions are located on the 8a tetrahedral sites and the 16d octahedral sites of the structure, respectively.[1,2] In the 4 V region, it appears that the cubic structure of the material is maintained during the extraction and insertion of Li^+ ions, but the capacity of the spinel electrode slowly loses during cycling. Recently, Tarascon and Guyomard[3] reported that lithium-rich spinel ($Li_{1+x}Mn_2O_4$) showed excellent cyclability at room temperature. However, a poor performance of the material at high temperature prevents its wider use as cathode material for lithium secondary batteries. For commercial use, the high temperature performance of $LiMn_2O_4$ must be improved. To improve the cyclability of spinel $LiMn_2O_4$ electrodes at high temperature, many research groups have studied cation substitution for Mn, and anion (F) for O, and surface passivation treatment of $LiMn_2O_4$.[4-6] Surface passivation treatments of $Li_{1.05}Mn_{1.95}O_4$ particles coated with lithium borate glass and acetylacetone improved the performance of the material at 55°C to some degree owing to minimizing the $LiMn_2O_4$/electrolyte interface. Amatucci *et al.* reported that the cyclability of fluorine-doped spinel $LiMn_2O_{4-x}F_x$ at 55°C was improved to some extent because of a decreased Mn dissolution.[6] The main possible reason for such poor performance has been attributed largely to the solubility of $LiMn_2O_4$ spinel due to the formation of HF resulting from the reaction of fluorinated anions with residual H_2O.[7,8] Liu *et al.* reported that a significant amount of tetragonal $Li_2Mn_2O_4$ in $Li_xMn_2O_4$ electrode after 80 cycles at the 4 V region appeared when charged and discharged at a high rate between 3.5 and 4.5 V and its existence was the result of kinetic limitations at the electrode surface during fast intercalation.[9] It was subsequently shown by Thackeray and co-workers that evidence of tetragonal $Li_2Mn_2O_4$ phase on the $LiMn_2O_4$ particles surface at the end of discharge (above 3 V) was detected by transmission electron microscopy (TEM) imaging after a few high rate cycles.[10] The presence of Li_2MnO_3 and spinel compositions other than $LiMn_2O_4$ in cycled $Li_xMn_2O_4$ electrodes has been reported previously by Robertson and co-workers.[11] Cho and Thackeray suggested that a capacity fade for Li/$LiMn_2O_4$ cycled hundreds of times in the 4 V region at room temperature is ascribed to the formation of Li_2MnO_3 at the particle surface which is attributed to the dissolution of MnO from $Li_2Mn_2O_4$.[12] It is generally accepted that the capacity loss for the $LiMn_2O_4$ electrode in the 4 V region could be attributed largely to a slow dissolution of MnO at the spinel particle into electrolyte. However, there is no explicit experimental data for the structural degradation at the spinel particle surface after cycling at room temperature as well as high temperature to confirm many researchers' observation and suggestion that is associated with capacity loss. Recently, we reported that a new sulfur-doped spinel, $LiAl_{0.24}Mn_{1.76}O_{3.98}S_{0.02}$, could eliminate the effect of Jahn-Teller distortion and showed excellent cyclability in the 3, 4 V, and both the 3 and 4 V regions at room temperature.[13,14]

In this paper, we study the high-temperature (50 and 80°C) performance of $LiAl_{0.24}Mn_{1.76}O_{3.98}S_{0.02}$ in the 4 V region combined with the structural degradation at the spinel particle surface. X-ray diffraction (XRD) and high-resolution transmission electron microscopy (HRTEM) were used to investigate the cycling-induced phase transformation of individual spinel particles at high temperature.

Experimental

$LiAl_{0.24}Mn_{1.76}O_{3.98}S_{0.02}$ powders were prepared by a sol-gel method as reported in our previous work.[13] $Li_{1.05}Al_{0.24}Mn_{1.75}O_{3.85}S_{0.15}$ was a starting composition of $LiAl_{0.24}Mn_{1.76}O_{3.98}S_{0.02}$. The slight excess of Li was introduced to compensate for losses during calcination.

The Li/$LiAl_{0.24}Mn_{1.76}O_{3.98}S_{0.02}$ cell discharged to 3.0 V was allowed to equilibrate for 5 h at each operating temperature. After cooling the cell to room temperature, the $LiAl_{0.24}Mn_{1.76}O_{3.98}S_{0.02}$ electrode was removed from the cell and then dried for one day. Powder XRD (Rigaku, Rint-2000) using Cu Kα radiation was used to identify the crystalline phase of as-prepared powders and cycled electrodes at various temperatures. Rietveld refinement was then performed using the XRD data to measure lattice constants.

The chemical composition was determined by chemical analysis using an inductively coupled plasma (ICP). The chemical analysis was conducted three times for each sample and the accuracy of the measured data was less than ±3%. To evaluate the solubility of spinel, 0.4 g of powders was loaded into a Teflon container bag, followed by immersing into 4 mL 1 M $LiPF_6$ in ethylene carbonate/dimethyl carbonate (EC/DMC) (1:2 by volume) electrolyte, which was kept at room temperature, 50 and 80°C, respectively, for one week. The electrolyte separated from the powders was analyzed for the measurement of Mn content.

The particle morphology of $LiAl_{0.24}Mn_{1.76}O_{3.98}S_{0.02}$ powders before and after cycling at 80°C was observed using a field emission scanning electron microscope (FESEM, Hitachi Co., S-4100). Microstructures of individual oxide particles of the samples were also

* Electrochemical Society Active Member.
z E-mail: yksun@email.hanyang.ac.kr

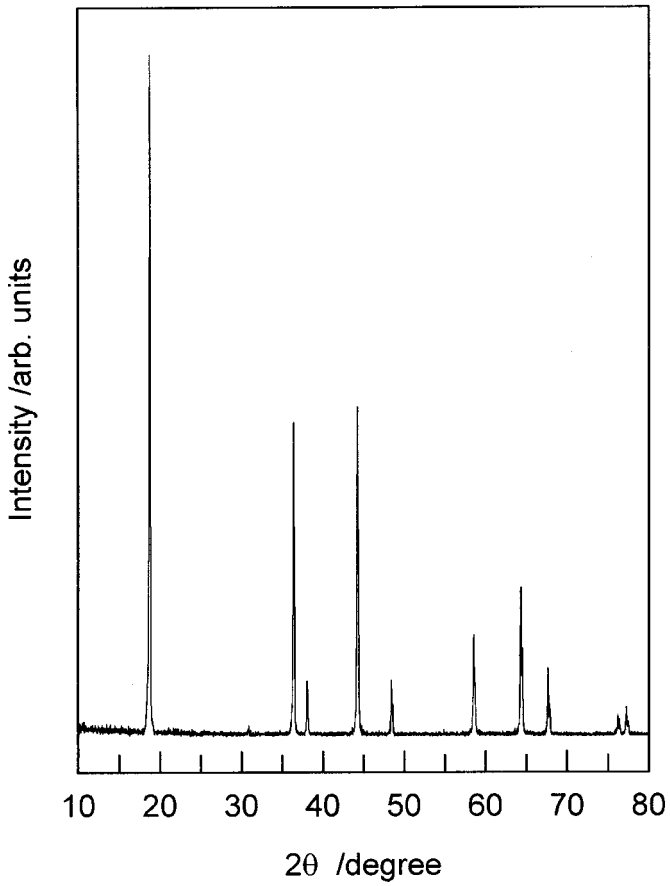

Figure 1. X-ray diffraction patterns for $LiAl_{0.24}Mn_{1.76}O_{3.98}S_{0.02}$ powders.

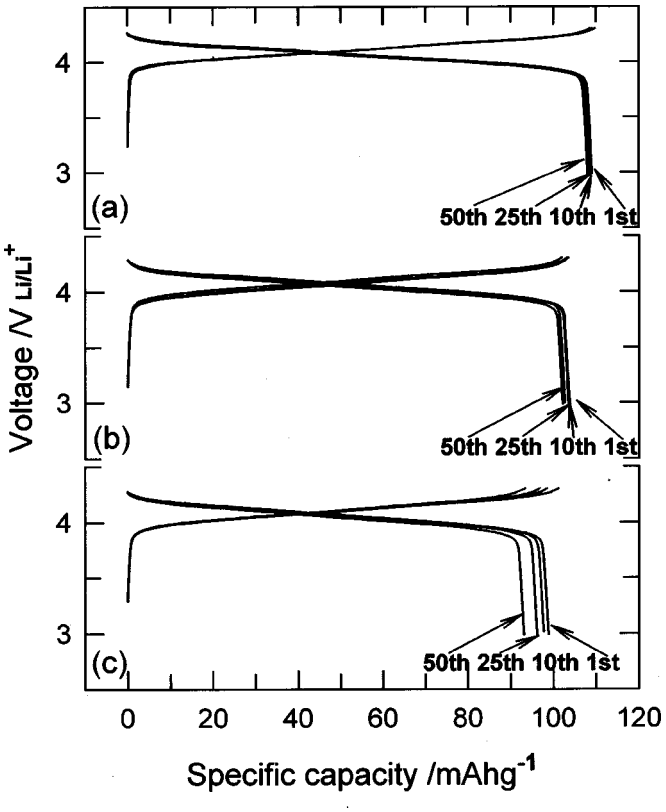

Figure 2. Charge-discharge curves for $Li/LiAl_{0.24}Mn_{1.76}O_{3.98}S_{0.02}$ cells at (a) room temperature, (b) 50, and (c) 80°C as a function of cycle number.

investigated by a TEM (H-9000NA), which uses an ultramicrotome technique[15] for specimen preparation.

Charge-discharge cycles were performed in CR2030 button-type cells. The cell consisted of a cathode and a lithium metal anode separated by a porous polypropylene film. For the fabrication of the electrode, the mixture, which contained 25 mg $LiAl_{0.24}Mn_{1.76}O_{3.98}S_{0.02}$ powders and 15 mg conducting binder (10 mg TAB and 5 mg graphite), was pressed on 2.0 cm^2 stainless screen at 800 kg/cm^2. The electrolyte used was a 1:2 EC/DMC mixture containing 1 M $LiPF_6$ by volume. The charge-discharge cycle was performed galvanostatically at a current rate of C/3 (0.4 mA/cm^2) between 4.3 and 3.0 V.

Results and Discussion

The as-prepared powders were confirmed to be well-defined spinel phase with space group $Fd3m$ shown in Fig. 1. There is a small 220 diffraction line ($2\theta = 30.4°$) which is generated by Li ion at 8a sites in the spinel host though the scattering factor of Li ions is very small. This indicates that as-prepared powders have higher crystallinity. The lattice constant (a) of the powders is 8.1928 Å which is lower than that of stoichiometric spinel.[7] The previous reports revealed that the lattice constant of metal-doped $LiM_xMn_{2-x}O_4$ spinel structures decreases with increasing amount of doped metal due to an increasing concentration of Mn^{4+} ions in the spinel structure by substituting Mn^{3+} ions with the metal ions.[16] The chemical analysis data showed the sample to be $LiAl_{0.24}Mn_{1.76}O_{3.98}S_{0.02}$ and the average oxidation state of manganese in the powders was 3.55.[13]

Figure 2 shows the charge-discharge curves for the $LiAl_{0.24}Mn_{1.76}O_{3.98}S_{0.02}$ electrode at room temperature, 50 and 80°C as a function of cycle number. The measured charge-discharge curves have only one plateau due to a large amount of Al substitution for Mn. While the polarization of the electrode at room temperature is almost constant during cycling, the polarization of the electrode cycled at 80°C increases with increasing cycle number. Shown in Fig. 3 is the variation of specific discharge capacity for the

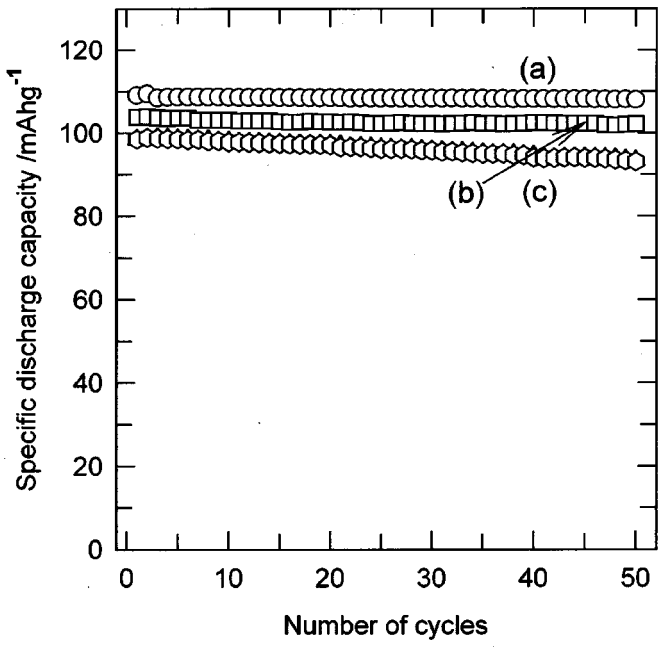

Figure 3. Variation of specific discharge capacities with number of cycles for the $Li/LiAl_{0.24}Mn_{1.76}O_{3.98}S_{0.02}$ cells at (a) room temperature, (b) 50, and (c) 80°C.

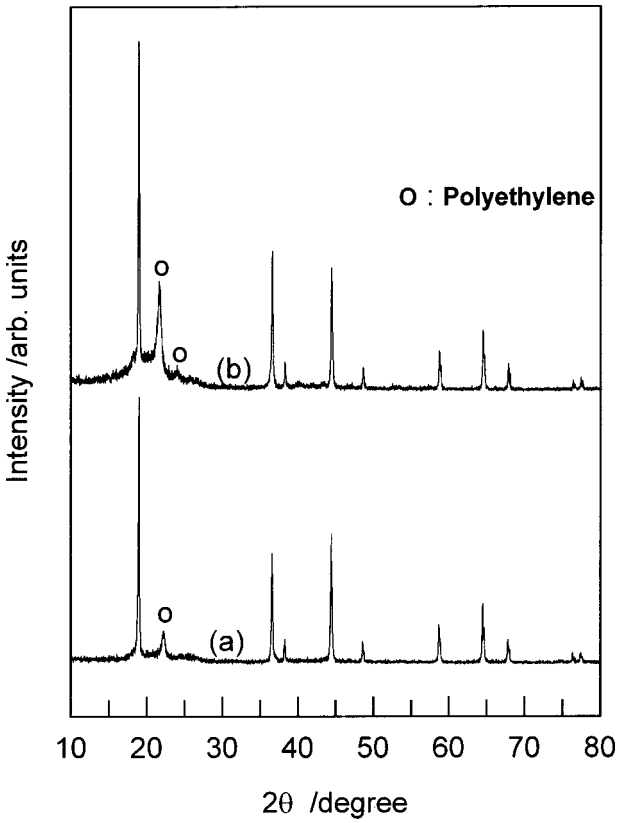

Figure 4. X-ray diffraction patterns for $LiAl_{0.24}Mn_{1.76}O_{3.98}S_{0.02}$ electrodes after 50 cycles at (a) 50 and (b) 80°C.

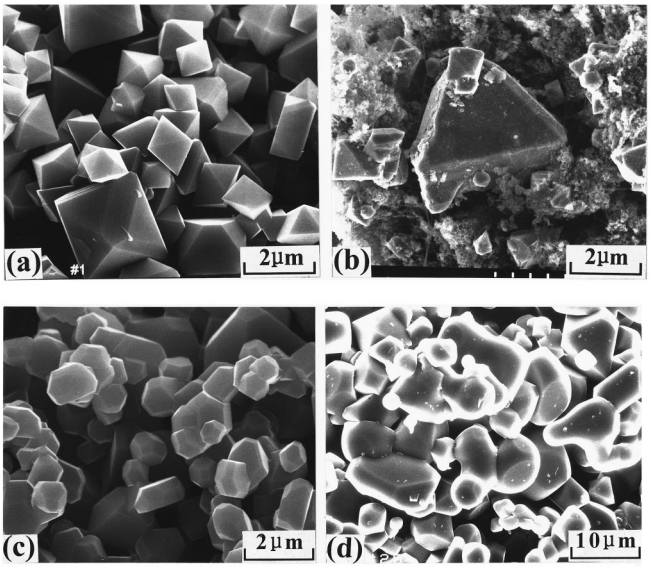

Figure 5. Scanning electron micrographs of the (a) $LiAl_{0.24}Mn_{1.76}O_{3.98}S_{0.02}$ powders, (b) electrode after 50 cycles at 80°C, and the as-prepared (c) $LiAl_{0.2}Mn_{1.8}O_4$ and (d) $LiMn_2O_{3.98}S_{0.02}$ powders.

oxysulfide electrodes during cycling at various temperatures. Although the electrode cycled at 25°C (Fig. 3a) delivers an initial capacity of 109 mAh/g, it shows excellent cycling behavior retaining 99% (0.020 mAh/g·cycle) of the initial capacity after 50 cycles at C/3 rate. While the capacity loss during cycling was a little faster at cell temperatures of 50 (Fig. 3b) and 80°C (Fig. 3c) than that of 25°C, the capacity retentions of the electrode at the temperatures of 50 and 80°C were 97 (0.024 mAh/g·cycle) and 95% (0.018 mAh/g·cycle) of the initial capacities of 104 and 99 mAh/g after 50 cycles, respectively. To our best knowledge, these are the lowest capacity losses observed at 50 and 80°C reported to date. This indicates that our prepared oxysulfide manganese oxides are a good cathode material which can compete with conventional cathode materials such as $LiCoO_2$ and $LiNi_{1-x}Co_xO_2$ for the application of high-temperature performance lithium batteries. The oxysulfide spinel oxide is an attractive cathode material for lithium secondary batteries due to temperature stability and excellent electrochemical performance as well as nontoxicity and low cost of raw materials.

Capacity loss during cycling has been commonly considered to be due to the Mn dissolution into the electrolyte solution. The as-prepared powders were first statically exposed in the electrolyte solution at room temperature, 50 and 80°C, respectively, for one week, and the dissolved Mn^{2+} ions in the electrolyte were analyzed. The dissolved amount of Mn^{2+} in the electrolyte is 5.6, 10.57, and 96.38 mg/L at room temperature, 50 and 80°C, respectively. It is noticeable that the amount of dissolved Mn at 80°C is nine times higher than that at 50°C.

To explore the cause of such poor capacity retention at the high temperature, XRD, SEM, and HRTEM were used to see the structure of the powders treated in the electrolyte at various temperatures. Figure 4 shows the XRD patterns for $LiAl_{0.24}Mn_{1.76}O_{3.98}S_{0.02}$ electrodes after 50 cycles at 50 and 80°C. When comparing XRD patterns for the cycled electrodes at 50 and 80°C (Fig. 4a and b) with that of the as-prepared powders (Fig. 1), we are unable to find any difference in the positions of the characteristic peaks for the typical spinel phase. The lattice constants of the electrodes cycled at 25, 50, and 80°C were 8.1778, 8.1682, and 8.1625 Å, respectively. Although there is very little difference in the lattice constants of the cycled electrodes at 50 and 80°C, the lattice constant difference between the as-prepared powders (8.1928 Å) and the cycled electrode at 80°C is large. Also, the lattice constants decrease with increasing cell operating temperatures, indicating an increase in the amount of Mn^{4+} and the decrease of crystallinity in the oxysulfide spinel due to Mn dissolution. As discussed above, the amount of Mn^{3+} decreases with increasing temperature because of a slow dissolution of spinels according to the disproportionation reaction; $2Mn^{3+} \rightarrow Mn^{4+} + Mn^{2+}$. The lower ionic radius of Mn^{4+} with respect to Mn^{3+} leads to higher covalency of the manganese-oxygen bonds and consequently to the decrease of the lattice constants of *a*.

Figure 5 shows SEM images of the as-prepared $LiAl_{0.24}Mn_{1.76}O_{3.98}S_{0.02}$ powders, the cycled electrode at 80°C, the as-prepared $LiAl_{0.2}Mn_{1.8}O_4$ and $LiMn_2O_{3.98}S_{0.02}$ powders. The particle morphology of as-prepared powders is analogous to that of single-crystal gold with a cubic structure. The particles are shaped into a well-developed polyhedra, mainly octahedral configuration bounded by eight (111) planes. The edge of the particle in the cycled electrode at 80°C is smoothed due to the Mn dissolution and/or surface structure change. The $LiAl_{0.24}Mn_{1.8}O_4$ and $LiMn_2O_{3.98}S_{0.02}$ powders are different from $LiAl_{0.2}Mn_{1.76}O_{3.98}S_{0.02}$ powders in morphology. Figure 5 reveals that the particles have intermediate shapes, changing from spherical to cubic octahedral structure. The particle sizes of $LiMn_2O_{3.98}S_{0.02}$ and $LiAl_{0.24}Mn_{1.76}O_{3.98}S_{0.02}$ are larger than those of $LiAl_{0.2}Mn_{1.8}O_4$ which do not contain sulfur ion in their structure. Especially, $LiMn_2O_{3.98}S_{0.02}$ has the particle size distribution of 5 $\sim$ 10 μm. At present, it is not clear how the size and morphology of particles affects the cycling behavior of the oxysulfide electrode. But we speculate that the excessively added sulfur may act as a catalyst in the synthetic process of S-doped Mn phase to enlarge the particle size.

To understand the phase transformation induced by the cycling at high temperature in detail, we conducted TEM analysis of the cycled electrode (the same material as shown in Fig. 4b) at 80°C in the fully discharged state and then compared the result with that of the as-prepared powders. Figure 6 shows a HRTEM micrograph ob-

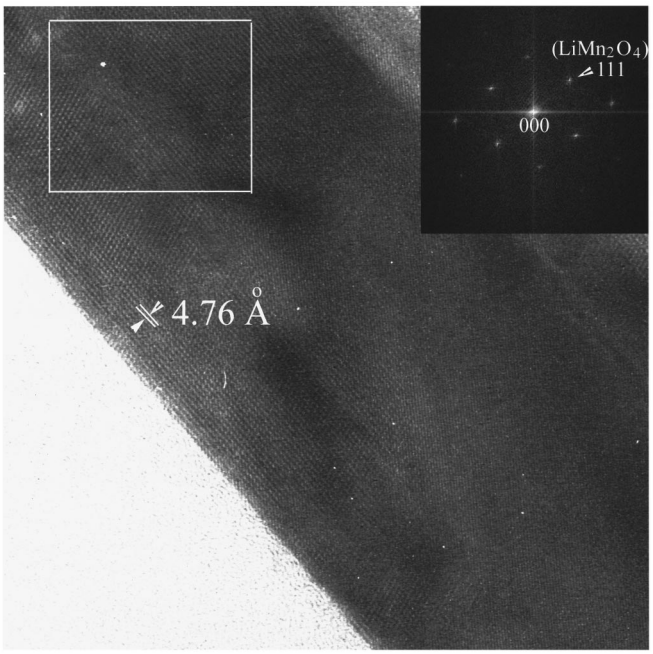

Figure 6. HRTEM lattice image and its digital diffractogram of $LiAl_{0.24}Mn_{1.76}O_{3.98}S_{0.02}$ powders.

tained from the surface of the as-prepared powders with its digital diffractogram. The lattice fringes of the as-prepared $LiAl_{0.24}Mn_{1.76}O_{3.98}S_{0.02}$ powders reveal a 0.476 nm modulation which is equivalent to the spacing of (111) plane in the cubic spinel structure. The lattices are not distorted, and the surface is smooth. Figure 7a shows a HRTEM micrograph obtained from the surface of the particles in the electrode after 50 cycles at 80°C. It is observed clearly that the surface roughness of the particle is irregular due to the structural change at the particle surface during cycling, suggesting that Mn dissolution leads to structural-transformed material at the surface of particles, while the cubic spinel phase is still in core. The thickness of structural change in the electrode after 50 cycles at 80°C is below 10 nm from the particle surface. To identify the changed structure of the particle surface, the analysis of the HRTEM image was carried out by the digital diffractograms and inverse Fourier transform filtered image.[17,18] Figure 7b demonstrates two digital diffractograms obtained from the framed areas A and B of Fig. 7a. The periodic components in the framed areas reveal themselves as diffraction spots in the diffractograms of Fig. 7b. The distance from the center to the diffracted spots indicates the reciprocal space. Indexing of the diffracted spots shown in Fig. 7b were performed by measuring the reciprocal spaces of the spots and the angles between the spots. It is found from the indexed results of the diffracted spots that two diffraction spots of area A correspond to the reflections of the $LiAl_{0.24}Mn_{1.76}O_{3.98}S_{0.02}$ with a cubic spinel structure, while the diffraction spots of area B correspond to the reflections of the Li_2MnO_3 and $LiAl_{0.24}Mn_{1.76}O_{3.98}S_{0.02}$ as shown in Fig. 7b. Figure 7c shows a processed image by the filtering method, where the image was obtained through inverse Fourier transform with 031 and 022 reflections of Li_2MnO_3, and 111 reflections of $LiAl_{0.24}Mn_{1.76}O_{3.98}S_{0.02}$. From the processed image, we can clearly see that the surface region of the spinel $LiAl_{0.24}Mn_{1.76}O_{3.98}S_{0.02}$ particles is partly changed into the Li_2MnO_3 with a rock salt phase. Further HRTEM lattice image for the $LiAl_{0.24}Mn_{1.76}O_{3.98}S_{0.02}$ electrode after 50 cycles at room temperature shows no formation of Li_2MnO_3 phase as shown in Fig. 8. Our data confirm Cho and Thackeray's speculation that the capacity loss in $Li/LiMn_2O_4$ cell is ascribed to a structural degradation of the spinel electrode which is

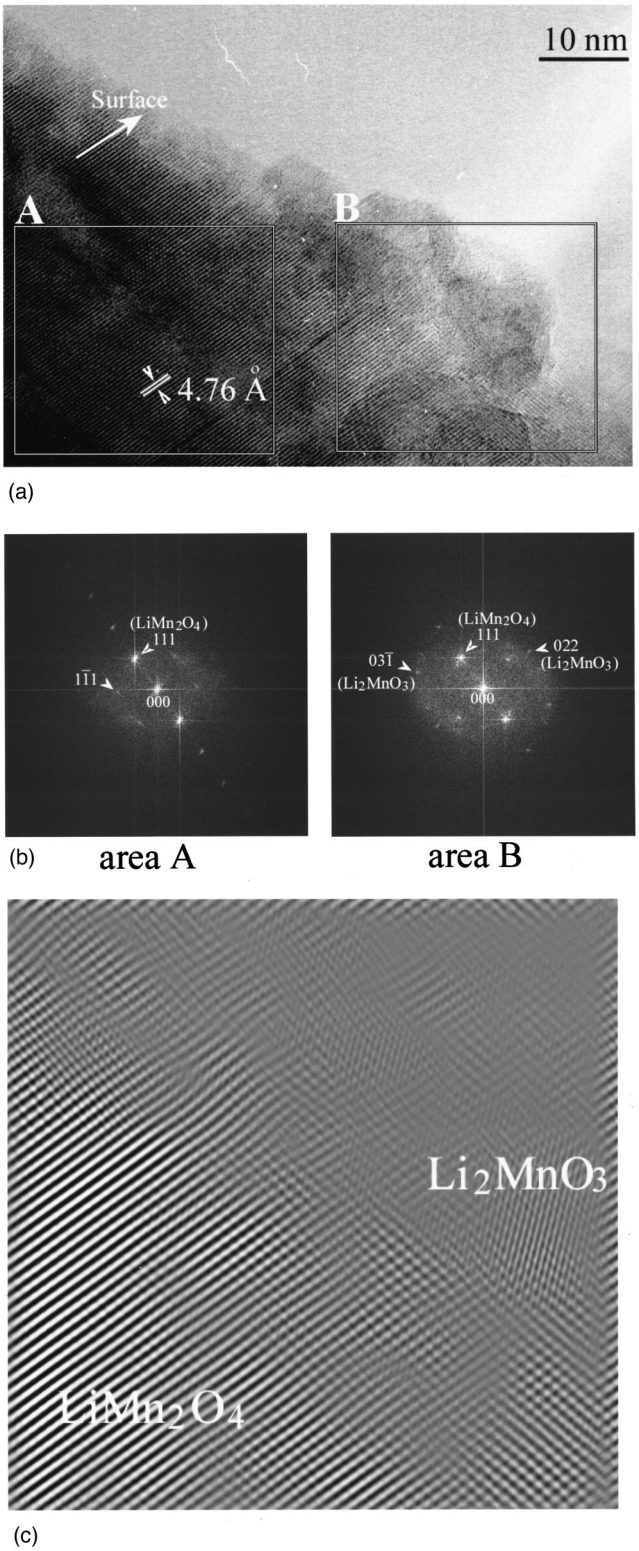

Figure 7. (a) HRTEM lattice image from particle surface in the electrode after 50 cycles at 80°C. A: Bulk region, B: Surface region. (b) Two digital diffractograms obtained from the framed areas A and B shown in a. (c) Filtering image of area A and B shown in a.

associated with the formation of Li_2MnO_3 resulting from the dissolution of MnO from $Li_2Mn_2O_4$. Thus, it is concluded that the formation of Li_2MnO_3 is due to the dissolution of MnO from $Li_2Mn_2O_4$

Figure 8. HRTEM lattice image from particle surface in the electrode after 50 cycles at room temperature.

formed on $LiAl_{0.24}Mn_{1.76}O_{3.98}S_{0.02}$ surface during cycling which results in the capacity loss of the oxysulfide spinel at high temperature. It is believed that the below 10 nm of structural change consisted of Li_2MnO_3 on the cycled electrode is responsible for the excellent cyclability for the oxysulfide spinel electrode after 50 cycles at 80°C.

Conclusions

An oxysulfide spinel, $LiAl_{0.24}Mn_{1.76}O_{3.98}S_{0.02}$, electrode cycled at high temperature shows excellent cyclability at a high rate over the 4 V region. The capacity retentions of the oxysulfide electrode after 50 cycles at room temperature, 50 and 80°C are 99, 97, and 95% of initial capacity of 109, 104, and 99 mAh/g, respectively. The rock salt Li_2MnO_3 phase was detected at the surface of discharged electrode after 50 cycles at 80°C by HRTEM imaging and the digital diffractograms. The excellent cyclability resulted from small structural degradation of the oxysulfide particle surface and the material could be used as an attractive cathode material in lithium secondary batteries.

Acknowledgment

The authors wish to acknowledge the financial support of the Korea Research Foundation made in the program year 2000.

Hanyang University assisted in meeting the publication costs of this article.

References

1. M. M. Thackeray, P. G. David, P. G. Bruce, and J. B. Goodenough, *Mater. Res. Bull.*, **18**, 461 (1983).
2. A. Yamada, K. Miura, K. Hinokuma, and M. Tanaka, *Mater. Res. Bull.*, **142**, 2149 (1995).
3. J. M. Tarascon and D. Guyomard, *J. Power Sources*, **54**, 92 (1995).
4. G. G. Amatucci, A. Bylr, C. Schmutz, and J. M. Tarascon, *Prog. Batteries Battery Mater.*, **16**, 1 (1997).
5. G. G. Amatucci, and J. M. Tarascon, U.S. Pat., 5,674,645 (1997).
6. G. G. Amatucci, A. Bylr, C. Siagala, P. Alfonse, and J. M. Tarascon, *Solid State Ionics*, **104**, 13 (1997).
7. D. H. Jang, Y. J. Shin, and S. M. Oh, *J. Electrochem. Soc.*, **143**, 2204 (1996).
8. D. H. Jang and S. M. Oh, *J. Electrochem. Soc.*, **144**, 3342 (1996).
9. W. Liu, K. Kowal, and G. C. Farrington, *J. Electrochem. Soc.*, **143**, 3590 (1996).
10. M. M. Thackeray, S. Yang, A. J. Kahaian, K. D. Kepler, E. Skinner, J. T. Vaughey, and S. A. Hackney, *Electrochem. Solid-State Lett.*, **1**, 7 (1998).
11. A. D. Robertson, S. H. Lu, and W. F. Howard, Jr., *J. Electrochem. Soc.*, **144**, 3505 (1997).
12. J. Cho and M. M. Thackeray, *J. Electrochem. Soc.*, **146**, 3577 (1999).
13. Y.-K. Sun, Y.-S. Jeon, and H. J. Lee, *Electrochem. Solid-State Lett.*, **3**, 7 (2000).
14. S. H. Park, K. S. Park, Y.-K. Sun, and K. S. Nahm, *J. Electrochem. Soc.*, **147**, 2116 (2000).
15. G.-S. Park, D. Shindo, Y. Waseda, and T. Sugimoto, *J. Colloid Interface Sci.*, **177**, 198 (1996).
16. D. Song, H. Ikuta, T. Uchida, and M. Wakihara, *Solid State Ionics*, **117**, 151 (1999).
17. G. S. Park and D. Shindo, *J. Electron Microsc.*, **45**, 152 (1996).
18. D. Shindo and K. Hiraga, *High-Resolution Electron Microscopy for Materials Science*, Springer, Tokyo (1998).